Biomed Tech 2008; 53:285–291 © 2008 by Walter de Gruyter • Berlin • New York. DOI 10.1515/BMT.2008.045

MRI-based inverse finite element approach for the mechanical assessment of patellar articular cartilage from static compression test

MRT-basierter Finite-Elemente-Ansatz zur mechanischen Beurteilung von patellarem Gelenkknorpel aus statischen Kompressionsversuchen

Sven Knecht[1,*], Roger Luechinger[2], Peter Boesiger[2] and Edgar Stüssi[1]

[1] Institute for Biomechanics, ETH Zurich, Switzerland
[2] Institute for Biomedical Engineering, University and ETH Zurich, Switzerland

Abstract

The mechanical property of articular cartilage determines to a great extent the functionality of diarthrodial joints. Consequently, the early detection of mechanical and, thus, functional changes of cartilage is crucial for preventive measures to maintain the mobility and the quality of life of individuals. An alternative to conventional mechanical testing is the inverse finite element approach, enabling non-destructive testing of the tissue. We evaluated a method for the assessment of the equilibrium material properties of the patellar cartilage based on magnetic resonance imaging during patellofemoral compression. We performed *ex vivo* testing of two equine patellas with healthy cartilage, one with superficial defects, and one with synthetically degenerated cartilage to simulate a pre-osteoarthritic stage. Static compression with 400 N for 2 h resulted in morphological changes comparable to physiological *in vivo* deformations in humans. We observed a decrease of the equilibrium Young's modulus of the degenerated cartilage by -59%, which was in the range of the results from indentation (-74%) and confined compression tests (-58%). With the reported accuracy of magnetic resonance imaging and its reproducibility, the results indicate the potential to measure differences in Young's modulus with regard to cartilage degeneration and consequently to distinguish between healthy and pre-osteoarthritic cartilage.

Keywords: articular cartilage; assessment; biomechanics; osteoarthritis.

Zusammenfassung

Die Funktionalität von diarthrodialen Gelenken wird in großem Maße von den mechanischen Eigenschaften des Gelenkknorpels bestimmt. Um die Mobilität und die Lebensqualität eines Menschen zu erhalten, ist es darum wichtig, frühzeitig Veränderungen der mechanischen Eigenschaften und somit der Funktionalität des Gelenkknorpels zu detektieren. Eine vielversprechende Alternative zu konventionellen mechanischen Tests bietet der inverse Finite-Elemente-Ansatz, mit dem zerstörungsfreies Prüfen des Gewebes ermöglicht wird. Wir haben diese Methode in Kombination mit der Magnetresonanztomographie während Kompressionstests an patellofemoralen Gelenken zur Beurteilung der mechanischen Eigenschaften von Gelenkknorpel evaluiert. Wir führten *Ex-vivo*-Tests an zwei Pferdekniescheiben mit gesundem Knorpel, einer mit defekter Knorpeloberfläche und einer mit künstlich degeneriertem Knorpel durch, um das präarthrotische Stadium zu simulieren. Statische Kompressionstests mit 400 N für 2 h führen zu ähnlichen morphologischen Veränderungen wie physiologische *In-vivo*-Deformationen beim Menschen. Wir beobachteten eine Abnahme des Young-Moduls beim degenerierten Knorpel um -59%, die in der Größenordnung der Ergebnisse aus den Indentationstests (-74%) und Kompressionstests (-58%) liegt. Diese Ergebnisse zeigen, dass aufgrund der Genauigkeit der Magnetresonanztomographie und der Reproduzierbarkeit diese Methode das Potenzial zur Ermittlung der Unterschiede des Young-Moduls hat, die mit der Degeneration von Knorpel einhergehen. Somit kann hiermit zwischen gesundem und präarthrotischem Knorpel unterschieden werden.

Schlüsselwörter: Arthrose; Beurteilung; Biomechanik; Gelenkknorpel.

Introduction

Articular cartilage (AC) plays a fundamental role for the functionality of diarthrodial joint. It protects the subjacent bone from high stresses and enables in combination with the synovial fluid a nearly frictionless movement over the whole lifespan of a person. The early detection of functional changes with regard to degenerative joint diseases, such as osteoarthritis (OA), is essential to prevent or reduce long-term disability [2, 5]. Since the functional behavior of AC is determined by the cartilage morphology and the mechanical properties, both parameters are appropriate to assess cartilage tissue. Magnetic resonance imaging (MRI) combined with state-of-the-art post-processing methods has shown its applicability to obtain accurate and highly reproducible quantitative data

*Corresponding author: Sven Knecht, Institute for Biomechanics, ETH Zurich, Wolfgang-Pauli Strasse 10, 8093 Zurich, Switzerland
Phone: +41-44-6336859
Fax: +41-44-6331124
E-mail: sven.knecht@gmail.com

of the morphology in healthy [6] and progressed osteoarthritic cartilage [8]. However, the biomechanical properties of AC seem to be more sensitive to pathological changes of the tissue as alterations of the structural and biochemical properties, determining the mechanical behavior, are one of the first events in AC degeneration [3]. As shown by Knecht et al. [14], measuring the cartilage static Young's modulus has the potential to identify early degenerative changes in AC. However, its reliable assessment *in vivo* fails up to now due to the lack of appropriate measurement techniques. Commonly used methods demand the excision of a well-defined cartilage sample [4] or invasive testing *in situ* [15]. Herberhold et al. [10] showed *ex vivo* that patellofemoral compression of human cadaveric knee with 1.5 times body weight (BW) for 3.5 h results in a local maximal deformation of the patellar cartilage thickness of 44% and a mean volumetric change of 29%. However, they did not assess the mechanical properties. In a preliminary study, we tested the *in vivo* applicability of an MR-compatible patellofemoral static compression test and showed a decrease of the global mean thickness of approximately 5% after loading with approximately 0.5 BW for 60 min [21]. This deformation from static compression was similar to dynamic *in vivo* results after knee bending [7]. The aim of the present study was to explore an MR-controlled patellofemoral compression test combined with an inverse finite element (FE) approach for the assessment of the equilibrium material properties of patellar AC.

Materials and methods

Patellofemoral compression test *in vitro*

Four equine joints were frozen and stored under -20°C within 8 h after death. They were defrosted overnight and dissected. The femoral counterpart of the patella was cut off (Figure 1B) and both parts were fixed with acrylic resin (Beracryl, Suter-Swiss composite, Fulenbach, Switzerland) in MR-compatible PE chambers (Figure 1C). The patellar sample was mounted onto the wooden lever of the compression device (Figure 1D). All tests were performed in 0.1 M phosphate-buffered saline (PBS).

We explored this approach using two healthy and visually intact, one superficially disrupted and one synthetically degenerated patellar cartilages (Table 1). Artificial degeneration was performed by treating the cartilage with a diluted solution of 1 mg/ml trypsin and 0.152 mg/ml EDTA×4 Na in Hanks' balanced salt (Gibco, Invitrogen, Basel, Switzerland) solution for 20 min at 37°C to simulate osteoarthritic cartilage [17]. Prior to the patellofemoral loading with 400 N for 2 h, all samples were equilibrated for 1 h in PBS.

Cartilage imaging was performed in the transversal plane using a 1.5-T MR scanner (Gyroscan Intera, Philips Medical System, Best, The Netherlands) and a surface microscopy coil (diameter 47 mm) with a spoiled 3D gradient echo sequence with water selective excitation (TR: 30 ms, TE: 7.4 ms, Flip angle: 20°, number of averages: 2). A 320×320 scan resolution with a field of view of 80 mm and a slice thickness of 1.4 mm results in a scan time of 7 min 42 s. Images were acquired before contact between the patellar and femoral cartilage was established (_pre), after load application (_00), after 2 h of creep test (_end), and 8 min after load removal (_post) (Figure 2).

Conventional mechanical assessment

The femoral and patellar samples were equilibrated after the patellofemoral compression test for 2 h in PBS to enable full recovery. Stress-relaxation indentation tests were performed at three positions on the medial and three on the lateral facet of the patella within the patellofemoral contact area. The patella was attached to a mechanical testing system (EnduraTec ELF 3200, Bose, Minnetonka, MN, USA) with a 22-N force cell (Honeywell Sensotec, Columbus, OH, USA). After a pre-load of 0.015 N for 60 s with a plane-ended circular indenter (diameter 0.99 mm), five displacement steps of 50 μm with a velocity of 5 μm/s up to a maximal deformation of 250 μm were conducted, and the resulting force was recorded for each of the six measurement sites. Cartilage thickness

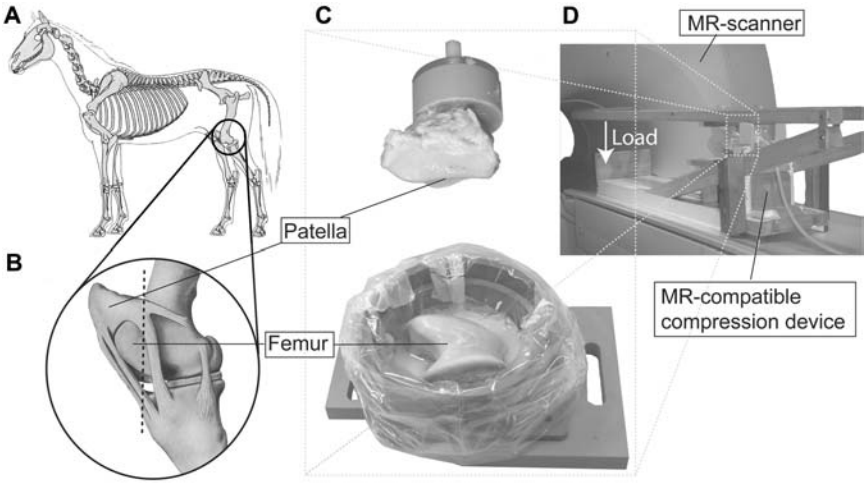

Figure 1 Sketch of the sample preparation from equine patellofemoral joints (A, B).
The femoral counterpart of the patella was cut at the dashed line (B) and fixed with acrylic resin in a PE chamber (C, bottom). Both components were attached to the MR-compatible compression device (D) and positioned in the MR scanner.

Table 1 Overview of the tested patellar cartilage samples.

Name	Sample	Condition of patellar cartilage	Applied load (N)
Comp1	Right patella	Healthy and intact surface	403
Comp2	Left patella	Healthy and intact surface	419
Comp3	Left patella	Superficially disrupted	419
Comp4	Right patella	Synthetically degenerated	411

was determined using a needle probe technique [12]. The equilibrium Young's modulus E was determined by a linear curve fit of the equilibrium stress-strain curve [20] with a Poisson's ratio of 0.1.

For confined compression tests, cartilage plugs were punched from locations next to the indentation testing site using a disposable skin biopsy punch (Stiefel Laboratorium, Offenbach, Germany) and removed from the subchondral bone. The plugs were tested in creep using the above-described testing system. Specimens were transferred into a smooth confining chamber (diameter 3.62 mm) and loaded with a porous sintered filter (diameter 3.54 mm, pore size 45 μm, porosity 45%; Schunk Sintermetalltechnik, Heuchelheim, Germany) in 0.1 M PBS. Strains of 5%, 10% and 15% were applied in a stepwise manner at a rate of 1 μm/s with 30 min relaxation time after each step. The aggregate modulus H_A was calculated by a linear curve fit of the equilibrium stress-strain curve. To determine the hydraulic permeability k, the experimental stress-relaxation curve for 5% strain was fitted with the theoretical solution by Soltz et al. [19] using a least squares algorithm in MATLAB (MathWorks, Inc., Natick, MA, USA).

Post-processing

Segmentation of the undeformed patellar and femoral cartilage and 3D reconstruction was performed using a custom-written software. For the reproducibility test, the data were segmented three times over a defined number of images with 1 week between the procedures. The polygonal surface models were imported into a commercial software package (Raindrop Geomagic, Geomagic Inc., Research Triangle Park, NC, USA) to fit non-uniform rational B-splines (NURBS) to the cartilage surface and the bone cartilage interface. The NURBS surfaces of the 3D geometries were imported into a commercial pre-processor (Patran 2005, MSC Software Corporation, Santa Ana, CA, USA) and meshed with linear 3D continuum elements (Figure 2, (8)). After registration of the images from the end and after load application with the undeformed data based on the bone cartilage interface (Figure 2, (3, 4)), the deformed cartilage geometries were segmented using the undeformed geometries as drafts. Translation and rotation of the geometries while establishing contact (_pre-_00) and during compression test (_00-_end) were determined by registration and implemented into the FE model to obtain precise models of the contact conditions at the beginning and the end of the compression test (Figure 2, (6, 7)). The point cloud of the patellar surface nodes at equilibrium was registered based on the undeformed bone cartilage interface to the initially undeformed FE mesh of the patellar cartilage using an iterative closest point (ICP) algorithm (Figure 2, (9)), programmed in MATLAB.

Quantitative data

Global morphological data, such as mean thickness, maximal thickness, and volume were calculated for the samples before load application, at the end of the compression and 8 min after load removal. Contact of the patellofemoral joint was defined when the distance between patellar and femoral surface was smaller than the in-plane resolution. Multiplication of the length of the contact with the slice thickness and their summation over all slices results in the total contact area [9]. Simplistic assumption that the volumetric deformation ΔV only occurs at the contact area A, divided by the undeformed mean thickness h_{mean} results in a mean strain $\varepsilon_{\text{mean}}$

$$\varepsilon_{mean} = \frac{\Delta V}{A^{*}h_{mean}} \tag{1}$$

This allows for calculation of a mean compressive modulus E_{mean} with the applied load P by

$$E_{mean} = \frac{P^{*}h_{mean}}{\Delta V} \tag{2}$$

Three-dimensional deviations of the undeformed and deformed patellar cartilage were determined using Geomagic Qualify (Geomagic Inc.) and displayed gray-scale-coded.

Inverse finite element approach

Large displacement contact analysis with frictionless small sliding was used with ABAQUS 6.5.4 (ABAQUS Inc., Pawtucket, RI, USA). The femoral bone cartilage interface nodes were fixed in all six directions, whereas the patellar bone cartilage interface nodes were kinematically coupled to a reference node outside the object. The load was applied linearly in one step within 2 s onto this reference node. AC was modeled as isotropic linear elastic material. This simplification is valid since the fluid flow was ceased in the tissue for the herein performed equilibrium test. Calculations were performed on a dual processor PC (Xeon CPU 3.4 GHz, 2 GB RAM). The difference between the two surfaces, defined as the distance between each predefined cartilage surface node of the FE calculation and its closest node on the surface of the experimental point cloud, was minimized using a non-linear least squares optimization algorithm in MATLAB. The robustness of the optimization algorithm and the sensitivity of the segmentation, registration and loading error were performed for one representative patellar

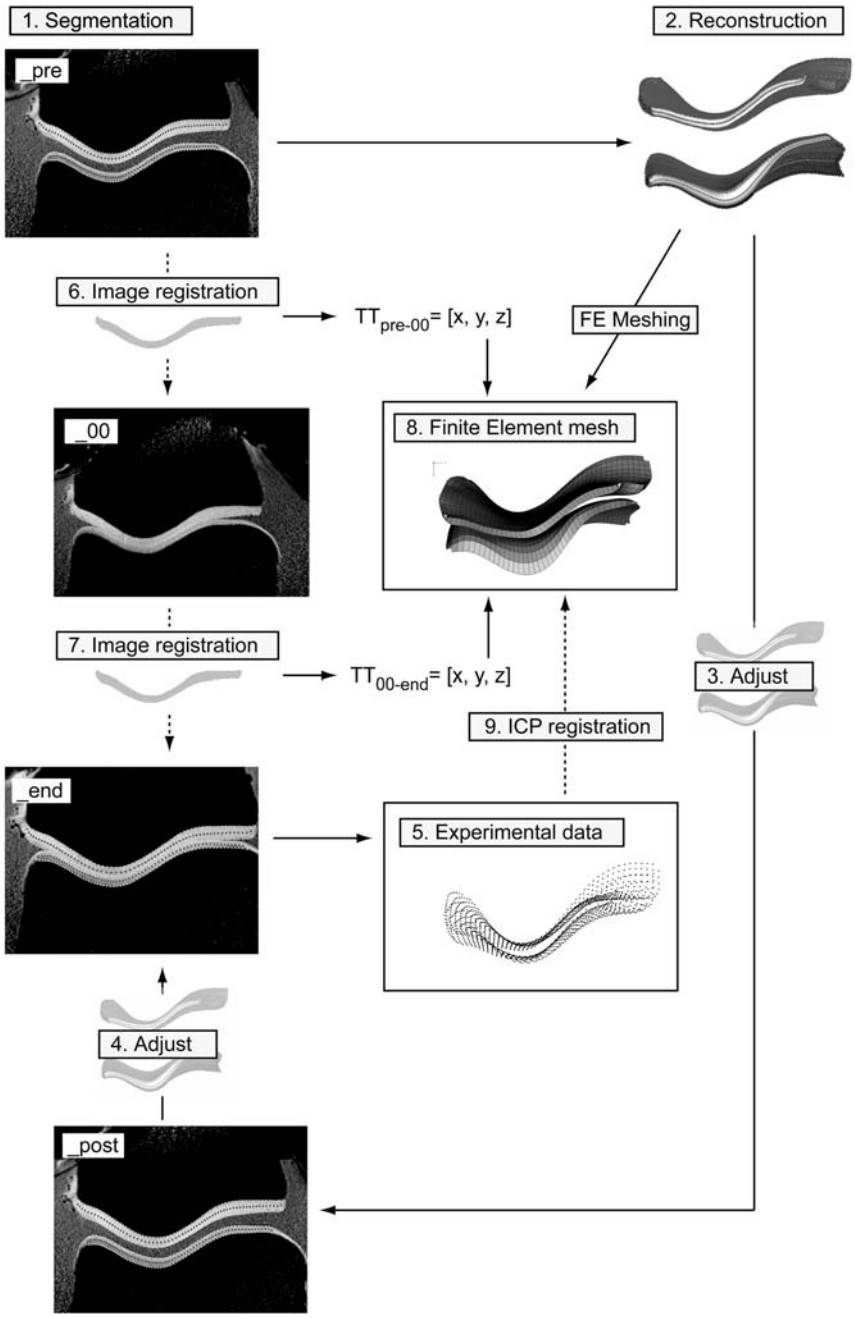

Figure 2 Flowchart of the entire pre-processing step to obtain the experimental data (5) and generate the FE model (8). Unloaded patellar and femoral cartilage were segmented (1), reconstructed using NURBS (2), meshed and imported into a FE software (8). The segmented geometry was used to segment the patellar cartilage after load removal (_post) and at the end of the compression test (_end). The point cloud of the patellar surface nodes at the end of the test (5) was registered based on the undeformable bone-cartilage interface to the undeformed FE mesh using an ICP algorithm (9).

geometry with an E_{FE} value of 2 MPa for six randomly generated starting values.

Statistical analysis

Values of the quantitative data were displayed as mean $\pm$ standard deviation (SD). The coefficient of variation (CV%) was calculated as standard deviation $\times$ 100 divided by the average value for the reproducibility test of the segmentation process and divided by the exact value for the assessment of the inverse FE approach. The mechanical properties from conventional mechanical testing were analyzed statistically using a two-way analysis of variance in Systat (Systat Software Inc., San Jose, CA, USA) with a significance level of $p = 0.05$.

Results

Conventional mechanical assessment

The values of the equilibrium properties were independent of the side (medial/lateral) for both healthy and degenerated cartilage. For healthy patellar cartilage, the

Table 2 Summary of the calculated mechanical properties of patellar articular cartilage for the four samples.

Sample	Method indentation E (MPa)	Confined compression H_A (MPa)	Patellofemoral compression	
			Inverse FE E (MPa)	Volumetric E_{mean} (MPa)
Comp1	1.669±0.496	n.d.a.	5.541	4.7
Comp2	1.374±0.305	0.568±0.130	5.627	4.8
Comp3	1.604±0.199	0.522±0.199	4.636	4.9
Comp4	0.400±0.053	0.228±0.094	2.176	1.8

All material properties were calculated using the linear elastic homogeneous isotropic material model and are displayed as mean±SD of all six measurements (three medial and three lateral). n.d.a., no data available.

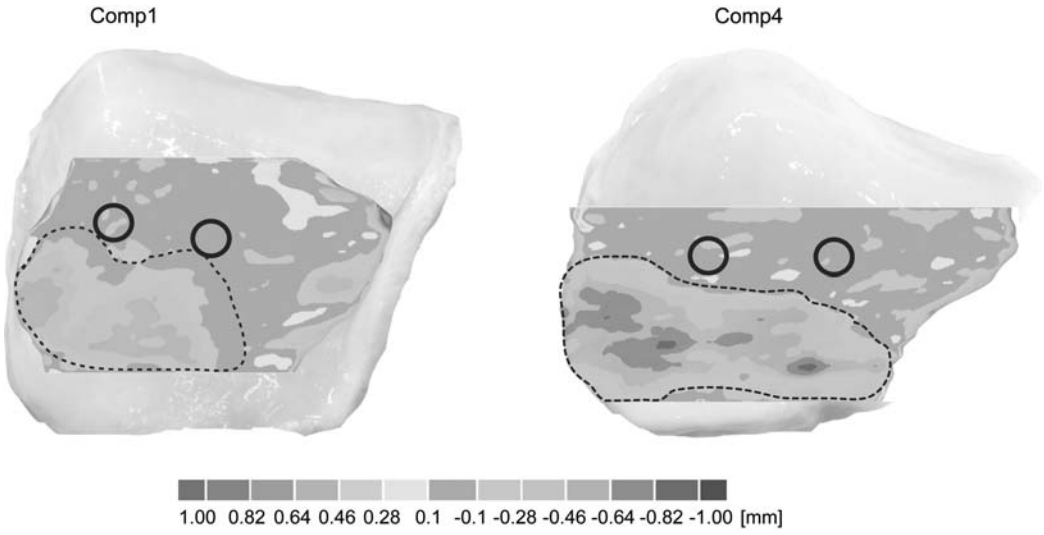

Figure 3 Exemplary views of the cartilage deformation of test Comp1 (intact) and Comp4 (synthetically degenerated). Deformation after 2 h of static compression with a load of approximately 400 N is displayed grayscale-coded. Dashed line represents the patellofemoral contact area. Circles represent the locations of the conventional mechanical test.

equilibrium Young's modulus varied between 1.37 MPa and 1.67 MPa, and the mean aggregate modulus was around 0.53 MPa (Table 2). The Young's and the aggregate moduli of the degenerated cartilage were evidently different from the healthy cartilage, whereas the hydraulic permeability was not different.

Reproducibility of the segmentation

The mean thickness for a reconstructed patellar cartilage was 2.03±0.02 mm, the maximal thickness was 2.94±0.05 mm, and the volume was 4559±56 mm^3. The CV% of these global morphological parameters was 0.84% for the mean thickness, 1.67% for the maximal thickness and 1.23% for the cartilage volume.

Deformational behavior

The mean thickness of the segmented patellar geometry decreased with compression between -3.67% and -5.30% for the healthy and by around -9% for the degenerated cartilage. Within 8 min after load removal, the mean thickness increased to the initial thickness for Comp3. Maximal thickness showed neither a decreasing nor an increasing trend during compression or after load removal. Cartilage volume decreases by around 190 mm^3 for healthy and 477 mm^3 for the degenerated cartilage. As for mean thickness, the cartilage volume increased to the initial volume for the superficially disrupted cartilage sample. The approximately calculated mean compressive modulus E_{mean} was around 4.8 MPa for the healthy and 1.8 MPa for the degenerated patellas (Table 2).

3D comparison of the undeformed and the deformed patellar cartilage revealed a maximal local deformation at the cartilage surface of around -0.5 mm for healthy and -0.8 mm for degenerated AC (Figure 3).

Inverse finite element approach

The entire calculation lasts approximately 160 min for a mean number of 60 forward FE calculations in ABAQUS, each lasting approximately 100 s. The CV% of the calculated Young's modulus E_{FE} for different starting values was less than 2.2%.

Sensitivity analysis

Segmentation error showed a maximal error in the calculated Young's modulus of 3.1%. Realistic out-of-plane registration error of 0.2 mm resulted in a maximal error of 2.7%. An experimental load error of -5% (-20 N) resulted in an error for E_{FE} of less than 7%. Poisson's ratio error was around 10% for all analyses. Worst-case calculations implementing the segmentation error, registration errors of approximately 0.2 mm and an error in the

applied load of approximately 4 N resulted in a slight overestimation of the Young's modulus of ~3%.

Linear elastic material behavior

The Young's moduli E_{FE} and the Poisson's ratio are between 4.5 and 5.5 MPa for the healthy and around 2.2 MPa for the degenerated patella. The mean of E_{FE} and the Poisson's ratio of healthy cartilage were 5.268 ± 0.549 MPa and 0.103 ± 0.022, respectively (Table 2).

Discussion

The detection of cartilage changes, e.g., in the early degenerative stage OA is increasingly important to prevent or reduce incidence of long-term disability. We evaluated a novel approach for the assessment of the mechanical properties of the patellar AC, which shows a prevalence of OA similar to that in the tibiofemoral joint (35% and 45%, respectively) [16].

The static patellofemoral compression test with human physiological loads of 0.5 BW (~400 N) on excised joints resulted in obvious and physiological deformation of the cartilage surface (Figure 3). The mean thickness deformation was in the range of patellar cartilage in young individuals after 30 deep knee bends [11] and after 80 min of *in vivo* patellofemoral compression [21]. The volumetric changes for the intact patellar cartilage are well comparable to physiological deformation *in vivo* after 50 knee bends [7]. Furthermore, the detected mechanical parameters are in the range of the human cartilage properties [1] just as the morphological parameter [10, 11]. Thus, the used equine animal model was adequate to simulate static loading on human patellofemoral joints with physiological human loads. In accordance with Setton et al. [18], we observed that superficial defects might be detected based on relaxation behavior.

The mean compressive modulus from the quantitative morphological parameter was in the range of the moduli from the inverse FE approach. Analyzing the morphological deformational data of six human cadaveric knee joints from reference [10] with Eq. (2) resulted in comparable mean compressive moduli between 1.6 and 3.0 MPa.

FE calculations with a difference in the Young's moduli of 30% and the consecutive 3D comparison of the deformed geometries revealed deviations of the cartilage deformation by more than 100 μm for all healthy samples and by more than 125 μm for the degenerated sample. As the position for the cartilage boundary can be located from MR images within a 0.5-pixel size [13], the herein used in-plane image resolution of 0.25×0.25 mm^2 allows to distinguish between differences of the Young's moduli by 30%.

The sensitivity analysis of the presented inverse FE approach revealed that the Young's modulus was only slightly dependent on the applied load, the segmentation and the registration process. We suppose that the low sensitivity of the Young's modulus to the applied load allows the use of this method for an *in vivo* application even with a more vague loading condition than in the herein performed idealized *ex vivo* setup.

The Young's moduli from indentation tests are higher than in other published studies. However, we observed with all performed tests a decrease of the mechanical properties of the synthetically degenerated cartilage compared to the pooled healthy data (E=-74%, H_A=-58%, E_{FE}=-59%, E_{mean}=-62%). Thus, all mechanical tests and analyses seem to be applicable to detect differences in the mechanical properties between healthy and degenerated cartilage. To verify this assumption statistically, a higher number of specimens have to be tested.

Due to the large individual differences in Young's modulus between subjects, this method might be used for longitudinal studies to detect time-dependent degenerative or adaptive processes. It might be applicable to detect adaptive processes that come with physiotherapeutic treatments or changes in the loading regime. However, for further *in vivo* application, the loading apparatus has to be improved to allow for a more comfortable loading of the patellofemoral joint for at least 1 h.

In conclusion, we explored the sensitivity and accuracy of a novel MR-controlled patellofemoral compression test to detect mechanical changes *in situ*. The results indicate that this method may have potential to distinguish between patellar cartilage with differences in the Young's moduli between 20% and 30%, and consequently to distinguish between healthy and moderately degenerated AC in the early stage of the osteoarthritis process [14]. Furthermore, solely considering the morphological properties, statements about the intactness of the superficial zone and about an approximate estimate of the modulus of the cartilage might be possible. The adaptation of this method for the *in vivo* application may provide a novel approach to determine functional changes of AC noninvasively and quantitatively for the first time.

Acknowledgements

The authors thank Mr. Ivo Telley for his help and the International Society of Biomechanics (ISB) for financial support.

References

[1] Armstrong CG, Mow VC. Variations in the intrinsic mechanical properties of human articular cartilage with age, degeneration, and water content. J Bone Joint Surg Am 1982; 64: 88–94.

[2] Bjorklund L. "The bone and joint decade 2000–2010. Inaugural meeting 17 and 18 April 1998, Lund, Sweden". Acta Orthop Scand Suppl 1998; 281: 67–80.

[3] Buckwalter JA, Mankin HJ. Articular cartilage: degeneration and osteoarthritis, repair, regeneration, and transplantation. Instr Course Lect 1998: 47: 487–504.

[4] Buschmann MD, Soulhat J, Shirazi-Adl A, Jurvelin JS, Hunziker EB. Confined compression of articular cartilage: linearity in ramp and sinusoidal tests and the importance of interdigitation and incomplete confinement. J Biomech 1998; 31: 171–178.

[5] Cicuttini FM, Jones G, Forbes A, Wluka AE. Rate of cartilage loss at two years predicts subsequent total knee arthroplasty: a prospective study. Ann Rheum Dis 2004; 63: 1124–1127.

[6] Eckstein F, Gavazzeni A, Sittek H, et al. Determination of knee joint cartilage thickness using three-dimensional magnetic resonance chondro-crassometry (3D MR-CCM). Magn Reson Med 1996; 36: 256–265.
[7] Eckstein F, Tieschky M, Faber S, Englmeier KH, Reiser M. Functional analysis of articular cartilage deformation, recovery, and fluid flow following dynamic exercise in vivo. Anat Embryol (Berl) 1999; 200: 419–424.
[8] Eckstein F, Mosher T, Hunter D. Imaging of knee osteoarthritis: data beyond the beauty. Curr Opin Rheumatol 2007; 19: 435–443.
[9] Heino-Brechter J, Powers CM. Patellofemoral stress during stair ascent and descent in persons with and without patellofemoral pain. Gait Posture 2002; 16: 115–123.
[10] Herberhold C, Faber S, Stammberger T, et al. In situ measurement of articular cartilage deformation in intact femoropatellar joints under static loading. J Biomech 1999; 32: 1287–1295.
[11] Hudelmaier M, Glaser C, Hohe J, et al. Age-related changes in the morphology and deformational behavior of knee joint cartilage. Arthritis Rheum 2001; 44: 2556–2561.
[12] Jurvelin JS, Rasanen T, Kolmonen P, Lyyra T. Comparison of optical, needle probe and ultrasonic techniques for the measurement of articular cartilage thickness. J Biomech 1995; 28: 231–235.
[13] Kauffmann C, Gravel P, Godbout B, et al. Computer-aided method for quantification of cartilage thickness and volume changes using MRI: validation study using a synthetic model. IEEE Trans Biomed Eng 2003; 50: 978–988.
[14] Knecht S, Vanwanseele B, Stuessi E. A review on the mechanical quality of articular cartilage – implications for the diagnosis of osteoarthritis. Clin Biomech 2006; 21: 999–1012.
[15] Korhonen RK, Wong M, Arokoski J, et al. Importance of the superficial tissue layer for the indentation stiffness of articular cartilage. Med Eng Phys 2002; 24: 99–108.
[16] McAllindon T, Zhang Y, Hannan M, et al. Are risk factors for patellofemoral and tibiofemoral knee osteoarthritis different? J Rheumatol 1996; 23: 332–337.
[17] Niederauer GG, Niederauer GM, Cullen LC, Athanasiou KA, Thomas JB, Niederauer MQ. Correlation of cartilage stiffness to thickness and level of degeneration using a handheld indentation probe. Ann Biomed Eng 2004; 32: 352–359.
[18] Setton LA, Zhu W, Mow VC. The biphasic poroviscoelastic behavior of articular cartilage: role of the surface zone in governing the compressive behavior. J Biomechan 1993; 26: 581–593.
[19] Soltz MA, Ateshian GA. Experimental verification and theoretical prediction of cartilage interstitial fluid pressurization at an impermeable contact interface in confined compression. J Biomech 1998; 31: 927–934.
[20] Toyras J, Rieppo J, Nieminen MT, Helminen HJ, Jurvelin JS. Characterization of enzymatically induced degradation of articular cartilage using high frequency ultrasound. Phys Med Biol 1999; 44: 2723–2733.
[21] Vanwanseele B. Quantification of the influence of the absence of normal joint loading and movement on the articular cartilage in the joints of spinal cord injured patients. PhD thesis, ETH Zurich, Switzerland 2003.

Received December 17, 2007; accepted August 4, 2008